PARIS 2017

Why multiples do not contribute to deconvolution imaging

Kees Wapenaar, Joost van der Neut and Evert Slob

Summary
The question whether multiples are signal or noise is subject of ongoing debate. In this paper we consider correlation and deconvolution imaging methods and analyse to what extent multiples contribute to the image in these methods. Our starting point is the assumption that at a specific depth level the full downgoing and upgoing fields (both including all multiples) are available. First we show that by cross correlating the full downgoing and upgoing wave fields, primaries and multiples contribute to the image. This image is not true-amplitude and is contaminated by cross-talk artefacts. Next we show that by deconvolving the full upgoing field by the full downgoing field, multiples do not contribute to the image. We use minimum-phase arguments to explain this somewhat counterintuitive conclusion. The deconvolution image is true-amplitude and not contaminated by cross-talk artefacts.
The conclusion that multiples do not contribute to the image applies to the type of deconvolution imaging analysed in this paper, but should not be extrapolated to other imaging methods. On the contrary, much research is dedicated to using multiples for imaging, for example in full wavefield migration, resonant migration and Marchenko imaging.

Introduction

The question whether multiples are signal or noise is subject of an ongoing debate (Valenciano and Chemingui, 2015; Weglein, 2015; Verschuur and Berkhout, 2015). The aim of this paper is not to address this question in general, but to analyse how one specific imaging method deals with multiples. In particular, we analyse imaging based on deconvolving the full upgoing wave field by the full downgoing field (both including all multiples) at each depth level. Using minimum-phase arguments, we explain the somewhat counterintuitive conclusion that in this imaging method the multiples in the downgoing and upgoing fields do not contribute to the image.

Correlation and deconvolution imaging conditions

Consider downgoing and upgoing wave fields at a specific horizontal boundary $\partial\mathbb{D}_n$ in an inhomogeneous subsurface, related to sources at the acquisition surface $\partial\mathbb{D}_0$. We denote the downgoing and upgoing fields as $p^+(\mathbf{x},\mathbf{x}_S,t)$ and $p^-(\mathbf{x},\mathbf{x}_S,t)$, respectively, where $\mathbf{x}$ denotes the receiver position at $\partial\mathbb{D}_n$, $\mathbf{x}_S$ the source position at $\partial\mathbb{D}_0$, and where t denotes time. We assume that these fields properly contain all multiple reflections (i.e., all internal multiples, and, in case the upper surface is a free boundary, also the surface-related multiples). For the following discussion it is not important how these fields have been obtained. They can be decomposed measured wave fields [for example at the ocean bottom (Amundsen, 2001) or in a horizontal borehole (Bakulin and Calvert, 2006; Mehta et al., 2007)], or they can have been obtained with an advanced wave field extrapolation method [for example by model-driven two-way wavefield extrapolation and decomposition (Wapenaar and Berkhout, 1986), by applying a model-driven Bremmer series approach (Davydenko and Verschuur, 2017), or by data-driven Marchenko redatuming (Wapenaar et al., 2014)]. We obtain a correlation image from

$$\hat{R}(\mathbf{x},\mathbf{x}',t) = \int_{\partial\mathbb{D}_0} \mathrm{d}\mathbf{x}_S \int_0^\infty p^-(\mathbf{x},\mathbf{x}_S,t+t')p^+(\mathbf{x}',\mathbf{x}_S,t')\mathrm{d}t', \quad \text{followed by} \quad I_{\mathrm{corr}}(\mathbf{x}) = \hat{R}(\mathbf{x},\mathbf{x},t=0), \quad (1)$$

where $\hat{R}(\mathbf{x},\mathbf{x}',t)$, with $\mathbf{x}$ and $\mathbf{x}'$ both at $\partial\mathbb{D}_n$, stands for an estimate of the (redatumed) reflection response of the half-space below $\partial\mathbb{D}_n$. This standard imaging method works well for primary data, but for data with multiples it gives rise to cross-talk, as we illustrate below with an example. This cross-talk can be avoided by replacing the total downgoing field $p^+(\mathbf{x}',\mathbf{x}_S,t')$ by the direct arriving wave $p_{\mathrm{d}}^+(\mathbf{x}',\mathbf{x}_S,t')$. In that case a multiple-free image is obtained (Wapenaar and Berkhout, 1986). The most general method that accounts for the multiples in $p^+(\mathbf{x},\mathbf{x}_S,t)$ and $p^-(\mathbf{x},\mathbf{x}_S,t)$ is the deconvolution imaging method. In this case, solve

$$p^-(\mathbf{x},\mathbf{x}_S,t) = \int_{\partial\mathbb{D}_n} \mathrm{d}\mathbf{x}' \int_0^\infty R(\mathbf{x},\mathbf{x}',t-t')p^+(\mathbf{x}',\mathbf{x}_S,t')\mathrm{d}t', \quad \text{followed by} \quad I_{\mathrm{decon}}(\mathbf{x}) = R(\mathbf{x},\mathbf{x},t=0). \quad (2)$$

Here $R(\mathbf{x},\mathbf{x}',t)$, with $\mathbf{x}$ and $\mathbf{x}'$ both at $\partial\mathbb{D}_n$, stands for the exact reflection response of the inhomogeneous half-space below $\partial\mathbb{D}_n$ (assuming a homogeneous half-space above $\partial\mathbb{D}_n$). It needs to be resolved from the integral representation by multi-dimensional deconvolution (Wapenaar et al., 2000; Amundsen, 2001), after which the image is obtained by extracting the $t=0$ component for $\mathbf{x}'=\mathbf{x}$.

The main aspect we want to illustrate in this paper is that, although $p^+(\mathbf{x},\mathbf{x}_S,t)$ and $p^-(\mathbf{x},\mathbf{x}_S,t)$ contain all multiple reflections, only the direct wave in $p^+(\mathbf{x},\mathbf{x}_S,t)$ and the primary reflection in $p^-(\mathbf{x},\mathbf{x}_S,t)$ contribute to the deconvolution image $I_{\mathrm{decon}}(\mathbf{x})$. For the sake of the discussion it is sufficient to analyse the 1D situation. To this end, we replace the downgoing and upgoing fields by $p^+(z,z_0,t)$ and $p^-(z,z_0,t)$, respectively, where z denotes depth. Moreover, the imaging methods, formulated by equations (1) and (2), simplify to

$$\hat{R}(z_n,t) = \int_0^\infty p^-(z_n,z_0,t+t')p^+(z_n,z_0,t')\mathrm{d}t', \quad \text{followed by} \quad I_{\mathrm{corr}}(z_n) = \hat{R}(z_n,t=0) \quad (3)$$

for the correlation method, and, for the deconvolution method, solve

$$p^-(z_n,z_0,t) = \int_0^\infty R(z_n,t-t')p^+(z_n,z_0,t')\mathrm{d}t', \quad \text{followed by} \quad I_{\mathrm{decon}}(z_n) = R(z_n,t=0). \quad (4)$$

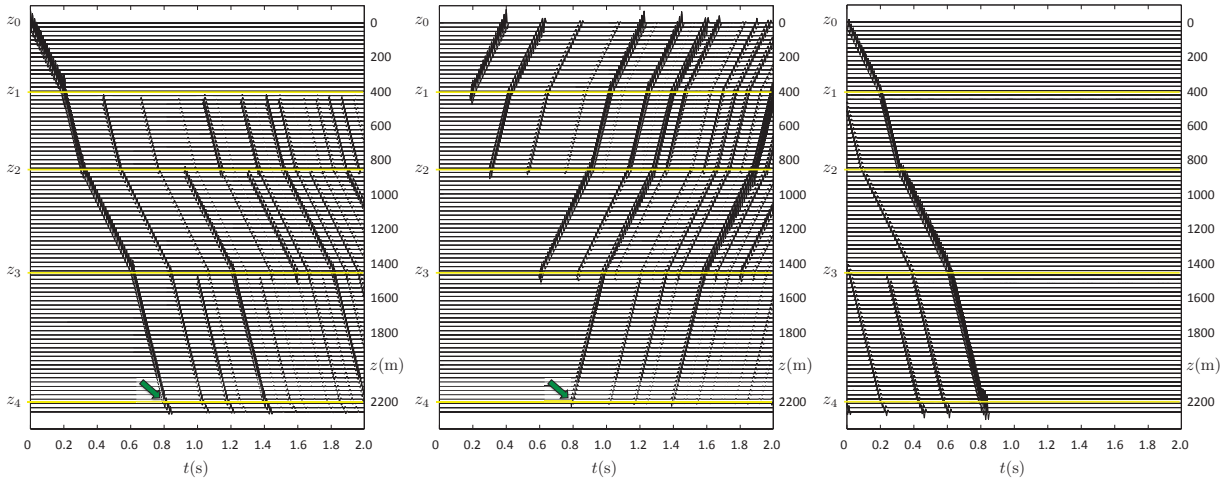

(a) (b) (c)

Figure 1 *(a) Downgoing field $p^+(z,z_0,t)$. (b) Upgoing field $p^-(z,z_0,t)$. (c) Time-reversed inverse downgoing field $p^+_{\text{inv}}(z,z_0,-t)$.*

Downgoing and upgoing fields in a horizontally layered medium

Consider a horizontally layered medium, consisting of four layers, enclosed between two homogeneous half-spaces. The propagation velocities of the four layers are $c_1 = 2000$, $c_2 = 4000$, $c_3 = 2000$, $c_4 = 4000$, all expressed in m/s, and the mass densities are $\rho_1 = 1000$, $\rho_2 = 2000$, $\rho_3 = 1000$, $\rho_4 = 2000$, expressed in kg/m^3. The depths of the layer boundaries are $z_0 = 0$, $z_1 = 400$, $z_2 = 850$, $z_3 = 1450$, $z_4 = 2200$, all expressed in m. The half-spaces above z_0 and below z_4 have a propagation velocity of 2000 m/s and a mass density of 1000 kg/m^3. The reflection coefficients of the four interfaces are $r_1 = 0.6$, $r_2 = -0.6$, $r_3 = 0.6$, $r_4 = -0.6$. Given a source for downgoing plane waves at the upper boundary z_0, the downgoing and upgoing fields $p^+(z,z_0,t)$ and $p^-(z,z_0,t)$ are shown in a VSP-like display in Figures 1(a) and (b). In this particular example these fields have been obtained from the reflection response $R(z_0,t)$, using the data-driven Marchenko method, but that is irrelevant for the remainder of this paper.

Correlation imaging

We consider correlation imaging, which we first illustrate for the fourth reflector, at $z = z_4$. From equation (3) we obtain (setting $t = 0$ and subsequently replacing t' by t)

$$I_{\text{corr}}(z_4) = \hat{R}(z_4,0) = \int_0^\infty p^-(z_4,z_0,t)p^+(z_4,z_0,t)\mathrm{d}t, \tag{5}$$

where depth level z_4 is considered to be approached from above. The traces $p^+(z_4,z_0,t)$ and $p^-(z_4,z_0,t)$, taken from Figures 1(a) and (b) just above $z = z_4$, are shown in Figures 2(a) and (b). The first events in these traces are the primary direct downgoing and the primary reflected wave, respectively (indicated by the green arrows in Figure 1). The other events are multiples. Equation (5) describes the zero-shift correlation of these traces. Figure 2 clearly shows that not only the primaries but also the multiples correlate (which is indicated by blue arrows). Hence, the multiples contribute to the correlation image $I_{\text{corr}}(z_4)$ (Behura et al., 2014). This may improve the signal-to-noise ratio, but the image is not a true-amplitude image. Moreover, evaluating equation (5) at other depth levels, the correlated multiples may give rise to ghost images. This is confirmed by Figure 3(a), which shows the correlation image $I_{\text{corr}}(z)$, obtained by evaluating the zero-shift correlation of the traces in Figures 1(a) and (b) for all z. The red arrow indicates a cross-talk artefact.
Artefacts such as those in Figure 3(a) do not occur when in the correlation process $p^+(z,z_0,t)$ is replaced by the direct downgoing field $p^+_{\text{d}}(z,z_0,t)$ (Wapenaar and Berkhout, 1986). This is not further discussed here.

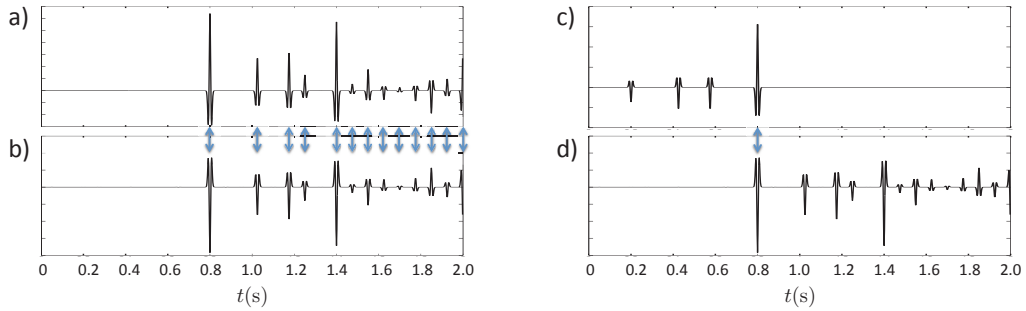

Figure 2 *(a) Downgoing field $p^+(z_4,z_0,t)$. (b) Upgoing field $p^-(z_4,z_0,t)$. The zero-shift correlation of these traces, expressed by equation (5), involves a sample-by-sample multiplication, followed by a summation over all samples, yielding the correlation image $I_{\rm corr}(z_4)$. Note that the primary as well as all multiples contribute to this image. (c) Time-reversed inverse downgoing field $p^+_{\rm inv}(z_4,z_0,-t)$. (d) Upgoing field $p^-(z_4,z_0,t)$. The zero-shift correlation of these traces, expressed by equation (7), yields the deconvolution image $I_{\rm decon}(z_4)$. Only the primary contributes to this image.*

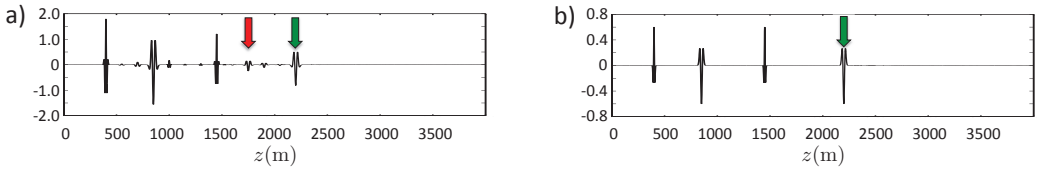

Figure 3 *(a) Correlation image $I_{\rm corr}(z)$ for all z. The green arrow indicates the image of the reflector at z_4, obtained from the zero-shift correlation of the traces in Figures 2(a) and (b). The red arrow indicates an artefact due to cross-talk. (b) Deconvolution image $I_{\rm decon}(z)$ for all z. The green arrow indicates the image of the reflector at z_4, obtained from the zero-shift correlation of the traces in Figures 2(c) and (d).*

Deconvolution imaging

Deconvolution imaging involves the inversion of the convolution integral in equation (4), followed by evaluating the $t=0$ component. The inversion of the convolution integral could be carried out as a two-step process: (1) evaluating the correlation, as described by equation (3), followed by (2) deconvolution for the autocorrelation of the downgoing wavefield. In the previous section we have seen that in step (1) the multiples give a contribution. Hence, intuitively one might think that they also contribute in this two-step process, particularly because the deconvolution in step (2) is done with a zero-phase signal. However, as we show now, the multiples do not contribute in deconvolution imaging. Defining $p^+_{\rm inv}(z_n,z_0,t)$ as the convolutional inverse of $p^+(z_n,z_0,t)$, we rewrite equation (4) as an explicit deconvolution process, according to

$$R(z_n,t)=\int_{-\infty}^{\infty} p^-(z_n,z_0,t-t')p^+_{\rm inv}(z_n,z_0,t')\mathrm{d}t', \quad \text{followed by} \quad I_{\rm decon}(z_n)=R(z_n,t=0). \tag{6}$$

We illustrate this for the fourth reflector at $z=z_4$. From equation (6) we obtain (setting $t=0$ and subsequently replacing t' by $-t$)

$$I_{\rm decon}(z_4)=R(z_4,0)=\int_{-\infty}^{\infty} p^-(z_4,z_0,t)p^+_{\rm inv}(z_4,z_0,-t)\mathrm{d}t. \tag{7}$$

Note that $p^+(z_4,z_0,t)$ is (apart from the transmission coefficient of the last interface), equal to the transmission response of the layered medium; hence, it is a causal minimum-phase signal, delayed by the direct arrival time $t_{\rm d}$ (Anstey and O'Doherty, 1971). The inverse of a minimum-phase signal is causal and minimum-phase as well (Robinson, 1954; Berkhout, 1974). Hence, $p^+_{\rm inv}(z_4,z_0,t)$ is a causal signal, advanced by $t_{\rm d}$. Equation (7) can be interpreted as a zero-shift correlation of the time-reversal of $p^+_{\rm inv}(z_4,z_0,t)$ and $p^-(z_4,z_0,t)$. These signals are shown in Figures 2(c) and (d). Note that only the primaries correlate (indicated by the blue arrow), and thus contribute to the deconvolution image $I_{\rm decon}(z_4)$. Clearly the multiples do not correlate and hence do not contribute to $I_{\rm decon}(z_4)$. The deconvolution image is a true-amplitude image ($r_4=-0.6$), see the event indicated by the green arrow in Figure 3(b).

For other depth levels, the downgoing field $p^+(z,z_0,t)$ can be written as a convolution of two minimum-phase functions (Wapenaar et al. (2013), equation 7). Hence, $p^+_{\rm inv}(z,z_0,t)$ is causal, advanced by $t_{\rm d}(z)$, and $p^+_{\rm inv}(z,z_0,-t)$ is acausal, delayed by $t_{\rm d}(z)$, for all z, which is confirmed by Figure 1(c). Figure 3(b) shows the deconvolution image $I_{\rm decon}(z)$, obtained by evaluating the zero-shift correlation of the traces in Figures 1(b) and (c) for all z. Note that this true-amplitude image contains no cross-talk artefacts.

Conclusions

Assuming the total downgoing and upgoing wave fields are available at a specific depth level, the multiples in these fields contribute to the image when applying correlation imaging, but the image is not true-amplitude and artefacts at other depth levels occur due to cross-talk. When applying deconvolution imaging, the multiples do not contribute, the image is true-amplitude and no cross-talk artefacts occur. We have used minimum-phase arguments to explain why only the primaries contribute to the deconvolution image.

This conclusion applies to the type of deconvolution imaging analysed in this paper, but should not be extrapolated to other imaging methods. For example, Verschuur and Berkhout (2015) and Davydenko and Verschuur (2017) show that multiples can be used in full wavefield migration. Guo et al. (2015) develop interferometric and resonant migration methods which employ information contained in multiples. Also in Marchenko imaging first results indicate that the deconvolution imaging condition can be modified such that multiples contribute to the image (Minato and Ghose, 2016; Wapenaar et al., 2017).

References

Amundsen, L. [2001] Elimination of free-surface related multiples without need of the source wavelet. *Geophysics*, **66**(1), 327–341.

Anstey, N.A. and O'Doherty, R.F. [1971] Reflections on amplitudes. *Geophysical Prospecting*, **19**, 430–458.

Bakulin, A. and Calvert, R. [2006] The virtual source method: Theory and case study. *Geophysics*, **71**(4), SI139–SI150.

Behura, J., Wapenaar, K. and Snieder, R. [2014] Autofocus Imaging: Image reconstruction based on inverse scattering theory. *Geophysics*, **79**(3), A19–A26.

Berkhout, A.J. [1974] Related properties of minimum-phase and zero-phase time functions. *Geophysical Prospecting*, **22**(4), 683–709.

Davydenko, M. and Verschuur, D.J. [2017] Full-wavefield migration: using surface and internal multiples in imaging. *Geophysical Prospecting*, **65**, 7–21.

Guo, B., Yu, J., Huang, Y., Hanafy, S.M. and Schuster, G.T. [2015] Benefits and limitations of imaging multiples: Interferometric and resonant migration. *The Leading Edge*, **34**, 802–806.

Mehta, K., Bakulin, A., Sheiman, J., Calvert, R. and Snieder, R. [2007] Improving the virtual source method by wavefield separation. *Geophysics*, **72**(4), V79–V86.

Minato, S. and Ghose, R. [2016] Enhanced characterization of fracture compliance heterogeneity using multiple reflections and data-driven Green's function retrieval. *Journal of Geophysical Research*, **121**, 2813–2836.

Robinson, E.A. [1954] *Predictive decomposition of seismic traces with applications to seismic exploration.* Ph.D. thesis, Massachusetts Institute of Technology.

Valenciano, A. and Chemingui, N. [2015] Introduction to this special section: Multiples from attenuation to imaging. *The Leading Edge*, **34**, 742.

Verschuur, D.J. and Berkhout, A.J. [2015] From removing to using multiples in closed-loop imaging. *The Leading Edge*, **34**, 744–759.

Wapenaar, C.P.A. and Berkhout, A.J. [1986] Wave-field extrapolation techniques for inhomogeneous media which include critical angle events. Part III: Applications in modeling migration and inversion. *Geophysical Prospecting*, **34**(2), 180–207.

Wapenaar, K., Broggini, F., Slob, E. and Snieder, R. [2013] Three-dimensional single-sided Marchenko inverse scattering, data-driven focusing, Green's function retrieval, and their mutual relations. *Physical Review Letters*, **110**, 084301.

Wapenaar, K., Fokkema, J., Dillen, M. and Scherpenhuijsen, P. [2000] One-way acoustic reciprocity and its applications in multiple elimination and time-lapse seismics. In: *SEG, Expanded Abstracts*. 2377–2380.

Wapenaar, K., van der Neut, J. and Slob, E. [2017] On the role of multiples in Marchenko imaging. *Geophysics*, **82**(1), A1–A5.

Wapenaar, K., Thorbecke, J., van der Neut, J., Broggini, F., Slob, E. and Snieder, R. [2014] Marchenko imaging. *Geophysics*, **79**(3), WA39–WA57.

Weglein, A.B. [2015] Primaries - The only events that can be migrated and for which migration has a meaning. *The Leading Edge*, **34**, 808–813.